

Towards highly efficient and highly transparent OLEDs: advanced considerations for emission zone coupled with capping layer design

Jin Chung,¹ Hyunsu Cho,^{1,2} Tae-Wook Koh,^{1,3} Jonghee Lee,² Eunhye Kim,¹ Jaeho Lee,¹ Jeong-Ik Lee,² and Seunghyup Yoo^{1,*}

¹Department of Electrical Engineering, Korea Advanced Institute of Science and Technology (KAIST), 373-1 Guseong-dong, Yuseong-gu, Daejeon 305-701, South Korea

²OLED Research Center, Electronics and Telecommunications Research Institute (ETRI), 218 Gajeong-ro, Yuseong-gu, Daejeon 305-700, South Korea

³Present address: Department of Electrical Engineering, Princeton University, Princeton, New Jersey 08540, USA
syoo@ee.kaist.ac.kr

Abstract: Strategies to achieve efficient transparent organic light-emitting diodes (TrOLEDs) are presented. The emission zone position is carefully adjusted by monitoring the optical phase change upon reflection from the top electrode, which is significant when the thickness of the capping layer changes. With the proposed design strategy, external quantum efficiency and transmittance values as high as 15% and 80% are demonstrated simultaneously. The effect of surface plasmon polariton (SPP) loss from thin metal electrodes is also taken into account to correctly describe the full scaling behavior of the efficiency of TrOLEDs over key optical design parameters.

©2015 Optical Society of America

OCIS codes: (230.3670) Light-emitting diodes; (230.4170) Multilayers; (310.4165) Multilayer design; (310.6845) Thin film devices and applications; (310.6860) Thin films, optical properties.

References and links

1. A. Buckley, *Organic Light-Emitting Diodes (OLEDs): Materials, Devices and Applications* (Woodhead Publishing, 2013), Ch. 17.
2. A. Poor, "Display week 2014 review: OLEDs," *Inf. Disp.* **30**(5), 10–13 (2014).
3. G. Gu, V. Bulović, P. E. Burrows, S. R. Forrest, and M. E. Thompson, "Transparent organic light emitting devices," *Appl. Phys. Lett.* **68**(19), 2606–2608 (1996).
4. A. Yamamori, S. Hayashi, T. Koyama, and Y. Taniguchi, "Transparent organic light-emitting diodes using metal acetylacetonate complexes as an electron injective buffer layer," *Appl. Phys. Lett.* **78**(21), 3343–3345 (2001).
5. M. Pfeiffer, S. R. Forrest, X. Zhou, and K. Leo, "A low drive voltage, transparent, metal-free n-i-p electrophosphorescent light emitting diode," *Org. Electron.* **4**(1), 21–26 (2003).
6. P. Görrn, M. Sander, J. Meyer, M. Kröger, E. Becker, H.-H. Johannes, W. Kowalsky, and T. Riedl, "Towards see-through displays: fully transparent thin-film transistors driving transparent organic light-emitting diodes," *Adv. Mater.* **18**(6), 738–741 (2006).
7. J. Meyer, T. Winkler, S. Hamwi, S. Schmale, H.-H. Johannes, T. Weimann, P. Hinze, W. Kowalsky, and T. Riedl, "Transparent inverted organic light-emitting diodes with a tungsten oxide buffer layer," *Adv. Mater.* **20**(20), 3839–3843 (2008).
8. J.-H. Lee, S. Lee, J.-B. Kim, J. Jang, and J.-J. Kim, "A high performance transparent inverted organic light emitting diode with 1,4,5,8,9,11-hexaazatriphenylenehexacarbonitrile as an organic buffer layer," *J. Mater. Chem.* **22**(30), 15262–15266 (2012).
9. J.-B. Kim, J.-H. Lee, C.-K. Moon, S.-Y. Kim, and J.-J. Kim, "Highly enhanced light extraction from surface plasmonic loss minimized organic light-emitting diodes," *Adv. Mater.* **25**(26), 3571–3577 (2013).
10. X. Zhou, M. Pfeiffer, J. S. Huang, J. Blochwitz-Nimoth, D. S. Qin, A. Werner, J. Drechsel, B. Maennig, and K. Leo, "Low-voltage inverted transparent vacuum deposited organic light-emitting diodes using electrical doping," *Appl. Phys. Lett.* **81**(5), 922–924 (2002).
11. S. Han, X. Feng, Z. H. Lu, D. Johnson, and R. Wood, "Transparent-cathode for top-emission organic light-emitting diodes," *Appl. Phys. Lett.* **82**(16), 2715–2717 (2003).
12. K. S. Yook, S. O. Jeon, C. W. Joo, and J. Y. Lee, "Transparent organic light emitting diodes using a multilayer oxide as a low resistance transparent cathode," *Appl. Phys. Lett.* **93**(1), 013301 (2008).

13. J. Lee, S. Hofmann, M. Furno, M. Thomschke, Y. H. Kim, B. Lüssem, and K. Leo, "Influence of organic capping layers on the performance of transparent organic light-emitting diodes," *Opt. Lett.* **36**(8), 1443–1445 (2011).
14. H. Cho, J.-M. Choi, and S. Yoo, "Highly transparent organic light-emitting diodes with a metallic top electrode: the dual role of a Cs₂CO₃ layer," *Opt. Express* **19**(2), 1113–1121 (2011).
15. J. W. Huh, J. W. Lee, D. Cho, J. Lee, and H. Y. Chu, "The optical effects of capping layers on the performance of transparent organic light-emitting diodes," *IEEE Photonics J.* **4**(1), 39–47 (2012).
16. J. W. Huh, J. Moon, J. W. Lee, D.-H. Cho, J.-W. Shin, J.-H. Han, J. Hwang, C. W. Joo, H. Y. Chu, and J.-I. Lee, "Directed emissive high efficient white transparent organic light emitting diodes with double layered capping layers," *Org. Electron.* **13**(8), 1386–1391 (2012).
17. C. S. Choi, D.-Y. Kim, S.-M. Lee, M. S. Lim, K. C. Choi, H. Cho, T.-W. Koh, and S. Yoo, "Blur-free outcoupling enhancement in transparent organic light emitting diodes: a nanostructure extracting surface plasmon modes," *Adv. Opt. Mater.* **1**(10), 687–691 (2013).
18. H.-W. Chang, J. Lee, T.-W. Koh, S. Hofmann, B. Lüssem, S. Yoo, C.-C. Wu, K. Leo, and M. C. Gather, "Bi-directional organic light-emitting diodes with nanoparticle-enhanced light outcoupling," *Laser Photonics Rev.* **7**(6), 1079–1087 (2013).
19. J. W. Huh, J.-W. Shin, D.-H. Cho, J. Moon, C. W. Joo, S. K. Park, J. Hwang, N. S. Cho, J. Lee, J.-H. Han, H. Y. Chu, and J.-I. Lee, "A randomly nano-structured scattering layer for transparent organic light emitting diodes," *Nanoscale* **6**(18), 10727–10733 (2014).
20. G. W. Kim, R. Lampande, J. Boizot, G. H. Kim, D. C. Choe, and J. H. Kwon, "An efficient nano-composite layer for highly transparent organic light emitting diodes," *Nanoscale* **6**(7), 3810–3817 (2014).
21. L. A. A. Pettersson, L. S. Roman, and O. Inganäs, "Modeling photocurrent action spectra of photovoltaic devices based on organic thin films," *J. Appl. Phys.* **86**(1), 487–496 (1999).
22. M. Furno, R. Meerheim, S. Hofmann, B. Lüssem, and K. Leo, "Efficiency and rate of spontaneous emission in organic electroluminescent devices," *Phys. Rev. B* **85**(11), 115205 (2012).
23. H. Cho, C. Yun, and S. Yoo, "Multilayer transparent electrode for organic light-emitting diodes: tuning its optical characteristics," *Opt. Express* **18**(4), 3404–3414 (2010).

1. Introduction

Organic light-emitting diodes (OLEDs) are considered a promising candidate for transparent displays that can lead to futuristic applications that are not readily available through conventional technologies – augmented reality, mutual interactive displays, and invisible displays seamlessly integrated with various objects, to name a few [1, 2]. Due to the transparency of the organic thin films used in OLEDs, transparent OLEDs (TrOLEDs) can be easily achieved by replacing their top, thick metal electrodes with a transparent one. A seemingly straight-forward transparent electrode for such a purpose may be transparent conductive oxides (TCOs), such as indium tin oxide (ITO) or indium zinc oxide (IZO) [3–9]; however, the sputtering deposition process used for TCOs can easily damage the underlying organic layers, making it difficult, though not impossible, to adopt them as a top electrode in TrOLEDs [4–9]. For this reason, thin metallic films (e.g. Ag or Au) have particularly been popular because they can be deposited by thermal evaporation with little damage to the underlying organic layers [10–12]. To improve the transmittance of the thin metal films, which exhibit finite visible-light transmittance typically in the range of 30% - 60%, many groups have suggested depositing dielectric capping layers (CL) on top of the thin metal layers [13–20]. For example, Lee et al. made a systematic study showing the influence of organic CL on the luminous current efficiency (CE), external quantum efficiency (EQE), and bottom-to-top intensity ratio. Huh et al. also discussed in detail the optical effects of CL on TrOLEDs, including the transmittance and emission spectra, and they proposed a useful guideline for the design of efficient TrOLEDs [15, 16, 19]. Most of these previous works, however, have focused only on the modulation of transmittance and concomitant resonance enhancement achieved by changes in CL thickness, leaving room for further improvement in the efficiency of TrOLEDs.

This work goes one step further and carefully monitors the changes in optical phase upon reflection from the top electrode when the CL thickness is varied and how this impacts the design of TrOLEDs for maximum efficiency and transmittance. Advanced optical simulations based on a classical dipole model are also used to describe the full scaling behavior with respect to a capping layer design, which also has an impact on loss to surface plasmon polariton (SPP) modes.

2. Experiments

TrOLEDs were fabricated on ITO-coated glass substrates (EVA SNP, Korea; $12 \Omega/\text{sq.}$). The substrates were cleaned sequentially with soapy water, deionized water, acetone, and isopropyl alcohol (IPA) and were subsequently treated by air plasma (PDC-32G, Harrick Plasma) for 5 min. Poly(3,4-ethylenedioxythiophene):poly(styrenesulfonate) (PEDOT:PSS; Clevis AI4083, Heraeus, Germany) was then spin-coated on top of ITO layers at 2000 rpm for 30 s, followed by drying at 120°C for 10 min on a hotplate. The samples were loaded into a thermal evaporator (HS-1100, Digital Optics & Vacuum), where all the other layers were deposited consecutively. Figure 1(a) depicts the fabricated device structures: ITO (150 nm)/ PEDOT:PSS (25 nm)/ MoO_3 (10 nm)/ 4,4'-bis(carbazol-9-yl)biphenyl (CBP) (35 nm)/ CBP doped with tris(2-phenylpyridine)iridium(III) ($\text{Ir}(\text{ppy})_3$, 8 wt.%) (15 nm)/ 4,7-diphenyl-1,10-phenanthroline (Bphen) (d_{emission})/ LiF (1 nm)/ Al (1 nm)/ Ag (15 nm)/ ZnS (d_{cap}).

The electrical and optical characteristics were measured in an N_2 -filled glove box using a customized measurement setup composed of a source-measure unit (Model 2400, Keithley), a calibrated Si photodiode (FDS-100-CAL, Thorlabs), a fiber-optic spectrometer (EPP 2000, StellarNet, Inc.), and a motorized rotation stage for goniometric measurement. The transmittance was measured using a UV-VIS spectrometer (SV2100, K-MAC).

The transmittance, reflectance, and phase change upon reflection were calculated with custom MATLAB codes based on transfer-matrix formalism [21]. Optical analysis for outcoupled modes, power dissipation into substrate modes, waveguided modes, and SPP modes was done based on an advanced classical dipole model that takes into account dipole orientation, Purcell effect, etc [22]. A thin sheet-like emission zone was assumed to be located at the interface between the emission layer (CBP: $\text{Ir}(\text{ppy})_3$) and the electron transport layer (Bphen) [22]. The optical constants of the materials used in calculations were measured by spectroscopic ellipsometry.

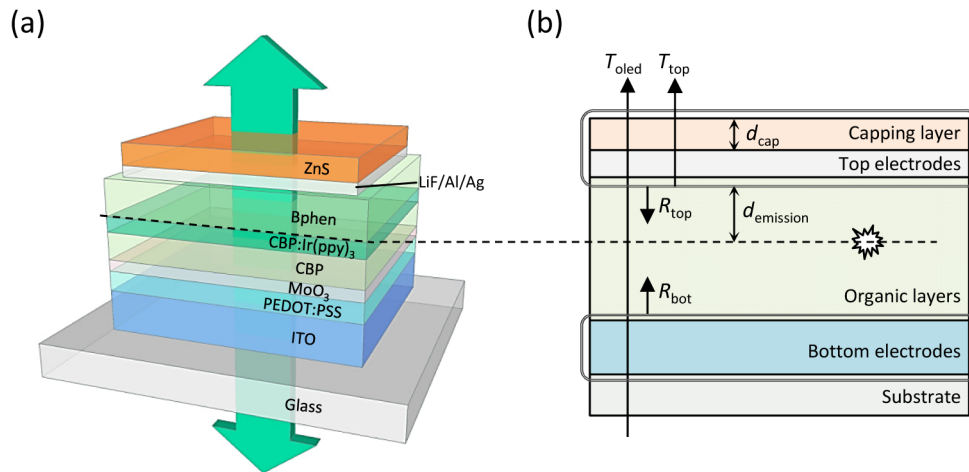


Fig. 1. (a) Device structure of the transparent OLEDs (TrOLEDs) under study with the thin metal (Ag) cathode and dielectric (ZnS) capping layer. (b) Schematic diagram of the simplified multilayer geometry of TrOLEDs with the local optical parameters.

3. Results and discussions

3.1 Effect of capping layer thickness on optical phase change and its implication for optimal emission zone location

In consideration of a OLEDs as a micro-cavity, its overall light output is determined by two major factors: (i) Fabry-Perot resonance enhancement due to multiple-beam interference and (ii) the two-beam interference effect, which is related to interference between directly emitted

light and reflected light [23]. In the case of TrOLEDs, however, device structures typically involve a transparent electrode on at least one side, and thus strong multiple-beam resonance is hardly expected due to low reflectance from the transparent electrode. It may still be important to consider the two-beam interference effect even in TrOLEDs, provided that one electrode is semitransparent and thus has a finite reflectance. For light with wavelength λ propagating along the symmetry axis, the two-beam interference factor (f_{TI}) is proportional to I_{out} or the axial light output toward a direction away from a semi-reflective electrode and is given by [23]:

$$I_{out} \propto f_{TI} = 1 + R_r + 2\sqrt{R_r} \cos(\Delta\phi_{TI})$$

$$\Delta\phi_{TI} = -\phi_r + \frac{4\pi n_{org} d_{emission}}{\lambda}$$
(1)

in which R_r and ϕ_r are the reflectance and the phase change for light reflecting from the semi-reflective electrode (e.g. top electrode for bottom emission or bottom electrode for top emission); n_{org} is the refractive index of organic layers, which is assumed, for simplicity, to be the same for all the organic layers involved; and $d_{emission}$ is the distance between the emission zone and the semi-reflective electrode. [See Fig. 1(b) for a summary of the terms used in Eq. (1).] In the top emission, the influence of f_{TI} on the I_{out} is small due to the low reflectance of the bottom ITO electrode ($R_r = R_{bot} \sim 1\%$ at organic/ITO interface from organic layer). However, f_{TI} can still be meaningful in the bottom emission due to relatively large reflectance of the top electrode ($R_r = R_{top}$), which typically consists of a thin metallic film covered with a dielectric capping layer.

The thickness of this capping layer (d_{cap}) can influence f_{TI} by changing T_{top} [R_{top}] and the effective phase change upon reflection (ϕ_{top}), as shown in Fig. 2(a) and 2(b), which present the calculated T_{top} , R_{top} , and ϕ_{top} of a top electrode structure based on a ZnS-capped thin Ag layer. It can be seen that T_{top} [R_{top}] exhibits sinusoidal modulation over d_{cap} as expected [11, 13]. For the 15-nm-thick Ag film, T_{top} [R_{top}] becomes the maximum [minimum] value at a d_{cap} of ~ 30 nm. It is noted that ϕ_{top} varies sensitively around d_{cap} leading to maximum T_{top} . The range of maximum variation in ϕ_{top} and its rate of change are aggravated when the thickness of Ag layer (d_{Ag}) decreases. For instance, when $d_{Ag} = 10$ nm, the maximum change in ϕ_{top} becomes as large as 0.87π (156°), and this significant change occurs when d_{cap} changes by only 6 nm from 19 nm to 25 nm. In fact, the optimal $d_{emission}$ ($= d_{emission}^{(opt)}$) maximizing f_{TI} , derived by setting $\Delta\phi_{TI}$ in Eq. (1) as the integer multiple of 2π , varies from 20 nm to 85 nm to compensate the 0.87π variation in ϕ_{top} for an OLED device with 10-nm-thick Ag covered with (22 ± 3) nm of d_{cap} . These tendencies suggest that the emission zone should be positioned carefully when one wishes to design highly transparent TrOLEDs by using a thin Ag layer and d_{cap} leading to maximum transmittance.

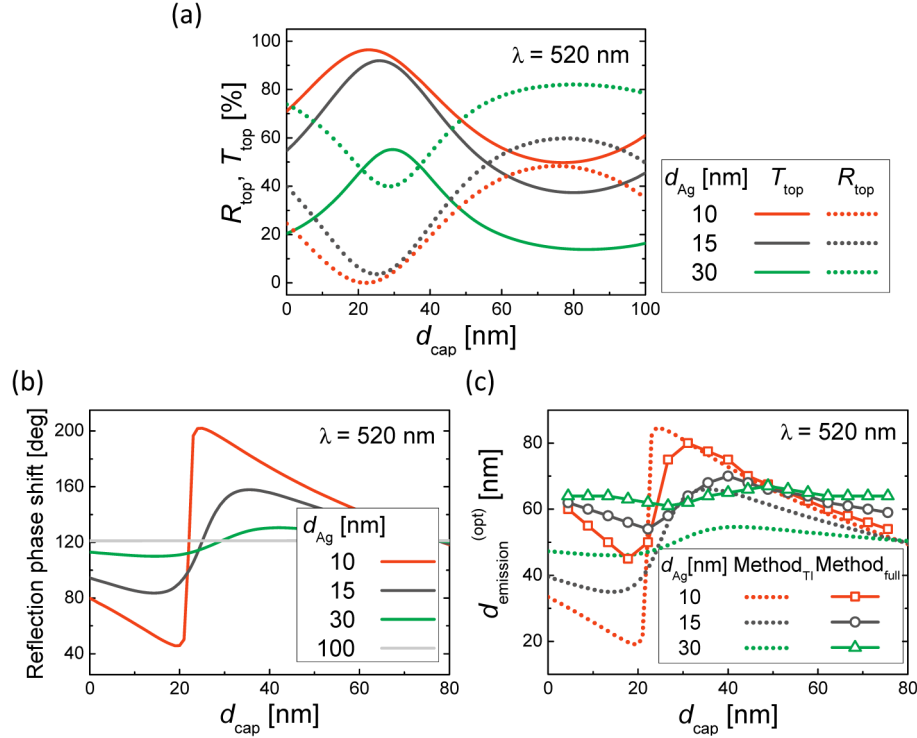


Fig. 2. (a) Calculated transmittance (T_{top}) and reflectance (R_{top}) at the top electrodes (composed of thin Ag and capping layer) and (b) the effective phase change upon reflection (ϕ_{top}) from top electrodes. (c) Calculated optimal location of emission zone ($d_{\text{emission}}^{\text{(opt)}}$) derived from two-beam interference effect (Method_{TI}) or from the classical dipole model (Method_{full}) [22].

While the discussion above illustrates well the significant influence of d_{emission} in conjunction with d_{cap} on f_{TI} , the scaling behavior of actual light output over d_{cap} and d_{emission} can be complicated due to subtle interplay among various loss mechanisms – waveguide and SPP modes as well as parasitic absorption. For more precise optical optimization, therefore, advanced optical simulation based on a classical dipole model has been used to obtain EQE as a function of d_{cap} and d_{emission} . In this model, the excitation of waveguided and SPP modes as well as the effect of the Purcell factor are fully taken into account [22]. Figures 3(a)-3(c) and Fig. 3(d) show the EQE for the top and bottom directions, total EQE, and the transmittance (T_{OLED} ; at the wavelength of 520 nm), respectively, calculated for an OLEDs device with d_{Ag} fixed at 15 nm. In this calculation, d_{cap} and d_{emission} are varied within a practically reasonable range [21], while the thicknesses of CBP as a hole transport layer (HTL) and CBP:Ir(ppy)₃ as an emitting layer (EML) are fixed at 35 nm and 15 nm, respectively.

It can be first seen that the EQE for the top direction ($= \text{EQE}_{\text{top}}$) is smaller than that for the bottom direction ($= \text{EQE}_{\text{bot}}$), as typically expected for TrOLEDs with an asymmetric electrode structure in which the bottom electrode has a lower reflectance than the top electrode [13, 15]. For this reason, the dependence of the total EQE ($= \text{EQE}_{\text{total}}$) on d_{cap} and d_{emission} is shown to be dominated by EQE_{bot} ; therefore, we focus on the trend of EQE_{bot} unless otherwise noted. It may also be noted that $\text{EQE}_{\text{total}}$ and EQE_{bot} depend more sensitively on d_{emission} than on d_{cap} , while T_{OLED} exhibits a slightly more sensitive dependence on d_{cap} than on d_{emission} , at least for a specific range of d_{cap} . The latter would be the case even for a wide range of d_{cap} , provided that the total thickness of organic layers was fixed. Such an opposite trend can be beneficial from a practical perspective in that one can adjust d_{cap} , more or less as a single independent parameter, to meet a target transmittance. Then, d_{emission} may be chosen for a given d_{cap} to maximize efficiency. This simplifies the overall design strategy and further

illustrates the importance of emission zone position obtained as a function of d_{cap} in TrOLEDs.

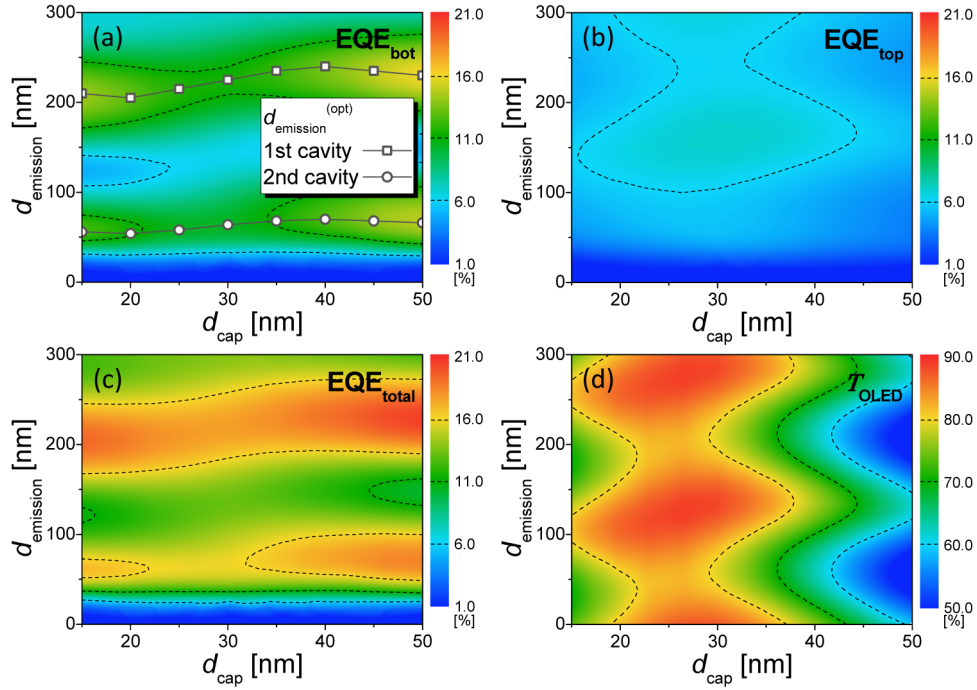


Fig. 3. Contour plots of calculated EQE and transmittance of transparent OLEDs as functions of emission zone position and capping layer thickness, according to the emission direction; (a) is EQE of bottom emission, (b) is the case of top emission, (c) is the sum of both directions, and (d) is transmittance at λ of 520 nm. The lines with symbol correspond to the optimal location of emission zone ($d_{\text{emission}}^{(\text{opt})}$) at the given d_{cap} derived from the classical dipole model (Method_{full}) [22].

As seen in the contour plots shown in Fig. 3(a), $d_{\text{emission}}^{(\text{opt})}$ yielding local maxima again varies in relation to d_{cap} for both 1st-order and 2nd-order cavity designs. However, it is noted that the range of $d_{\text{emission}}^{(\text{opt})}$ obtained in this way [= Method_{full}; shown as shapes in Fig. 2(c)] is not as wide as the range predicted from f_{TI} [= Method_{TI}; shown as lines in Fig. 2(c)]. For the 1st-order design, for example, the difference between the largest and smallest $d_{\text{emission}}^{(\text{opt})}$ [shown as circular shapes in Fig. 3(a)] is merely 16 nm (= 70 nm for d_{cap} of 40 nm minus 54 nm for d_{cap} of 20 nm) in Method_{full}, while it is ca. 31 nm (= 66 nm for d_{cap} of 35 nm minus 35 nm for d_{cap} of 14 nm) in Method_{TI}. Such a discrepancy is thought to come from SPP modes that take a significant portion when d_{emission} decreases to a value less than a few tens of nanometers. Indeed, Fig. 3(a)-3(c) clearly show that EQE values rapidly drop as d_{emission} becomes smaller than ca. 30 nm. The fact that the difference between the largest and smallest $d_{\text{emission}}^{(\text{opt})}$ for 2nd-order cavity TrOLEDs [shown as rectangular shapes in Fig. 3(a)] remains relatively large and becomes comparable to the value obtained with Method_{TI} is also consistent with such a notion because the role of SPP can decrease significantly in a 2nd-order cavity design.

The power dissipation spectra given as a function of in-plane wavevector (k_x) shown in Fig. 4(a) and 4(b) confirm that a significant amount of power dissipation exists at k_x even well beyond the boundary of k_x that divides propagating and evanescent modes (e.g. $22 \mu\text{m}^{-1}$ at λ of 520 nm or photon energy of 2.38 eV) in TrOLEDs with a small d_{emission} . The spectral power density at λ of 520 nm shown in Fig. 4(c) and 4(d) shows the dominant contribution of TM waves to these evanescent modes, being consistent with the fact that SPP modes are due to TM waves coupled with electron motion within metal.

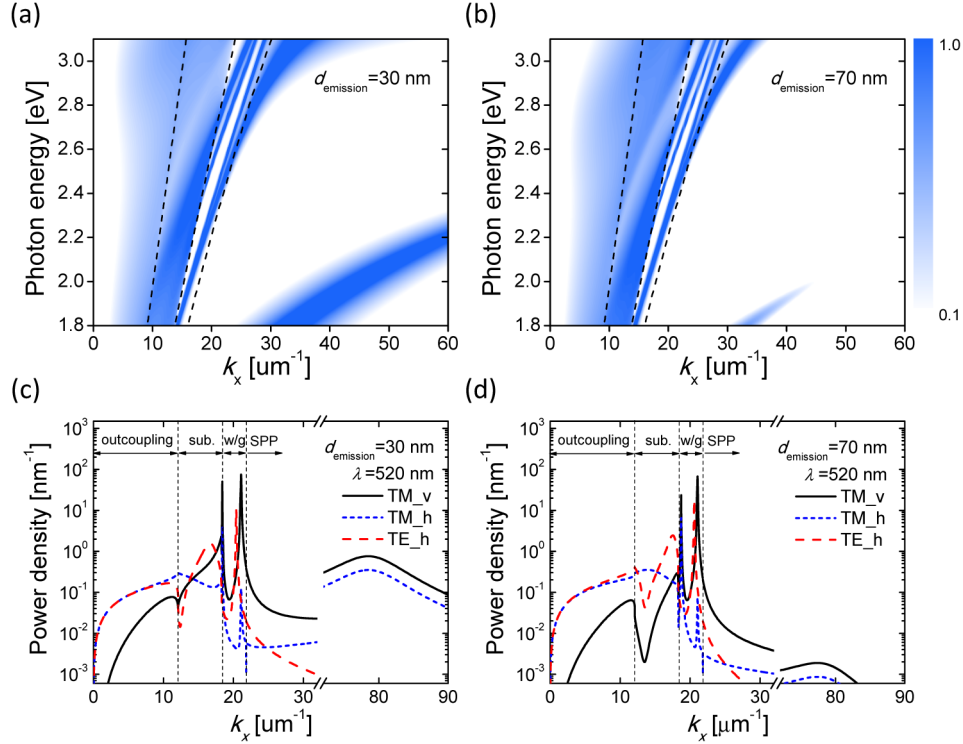


Fig. 4. Power dissipation spectra per unit of photon energy in the TrOLEDs with 40 nm-thick d_{cap} : for the case with (a) d_{emission} of 30 nm and with (b) 70 nm. Power dissipation spectrum at 2.38 eV ($\lambda = 520$ nm) according to dipole polarization in the TrOLEDs with (c) d_{emission} of 30 nm and (d) 70 nm. The dashed black line denotes the interface dividing the regions corresponding to outcoupled, substrate-confined, waveguided, and surface plasmon polariton (SPP) modes, respectively.

3.2 Device characteristics of transparent OLEDs

To demonstrate the role of d_{emission} in conjunction with top electrode design in TrOLEDs, working devices with d_{cap} values of 15 nm, 30 nm, and 40 nm were prepared with varying d_{emission} values. As seen in Fig. 5, all the fabricated TrOLEDs corresponded to a configuration yielding high transmittance, in which the device with a 30-nm-thick capping layer exhibited the highest and most balanced $T_{\text{OLED}}(\lambda)$ throughout the visible range. Those with 15 nm- and 40 nm-thick capping layers showed T_{OLED} values that were relatively high at red and blue parts of spectra, respectively. This range of d_{cap} leading to high T_{OLED} was chosen not only to achieve highly transparent OLEDs but also because the associated change in ϕ_{top} was shown to be the most significant in the thickness range leading to high T_{top} and thus high T_{OLED} in the previous section [see Fig. 2(a) and 2(b)]. To minimize complications from electrical characteristics, all the devices were prepared with a fixed total thickness of organic layers (110 nm) by adjustment of the HTL thickness to compensate the variation in d_{emission} . The current density (J) - voltage (V) characteristics of the TrOLEDs with a d_{cap} of 40 nm presented in Fig. 6(a) were virtually identical, regardless of the d_{emission} tried, supporting the idea that the difference in efficiency shown in Fig. 6(b) can be attributed mainly to the optical effect.

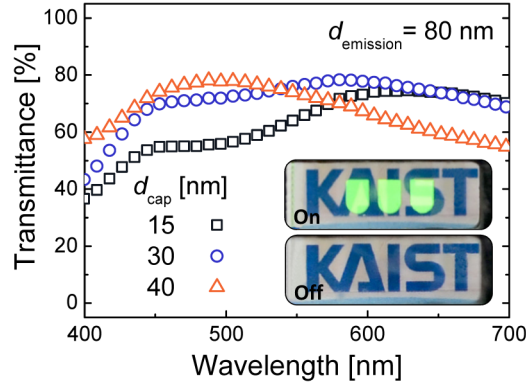


Fig. 5. Measured transmittance of transparent OLEDs according to the thickness of the capping layer (inset: the pictures of the proposed TrOLEDs with a 30-nm-thick capping layer in on and off states).

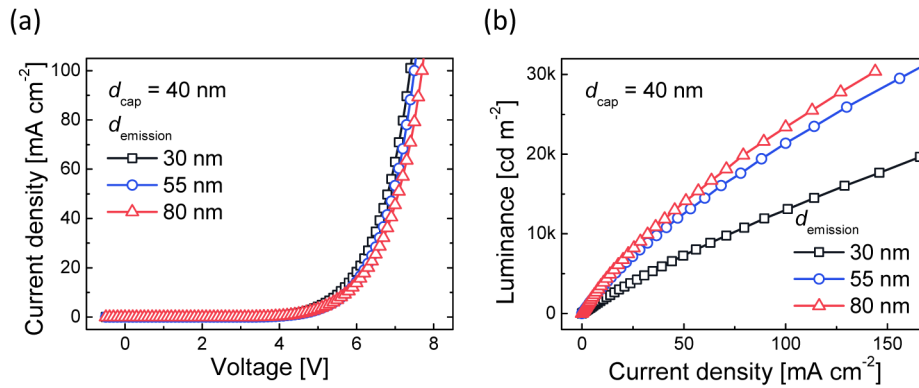


Fig. 6. (a) Current density-voltage (J - V) and (b) luminance-current density (L - J) characteristics of the TrOLEDs with 40-nm-thick capping layer in relation to emission zone position.

Figures 7(a)-7(c) present the measured and simulated EQE vs. d_{emission} for the TrOLEDs with varying d_{cap} values under study. The scaling behaviors of EQE_{bot} , EQE_{top} , and $\text{EQE}_{\text{total}}$ all match reasonably well to those predicted by advanced optical simulation (Method_{full}). This agreement over various cases can be regarded as especially meaningful since there is no adjustment parameter. The relative trend of EQE_{bot} predicted by f_{TI} (d_{cap} , d_{emission}) under Lambertian approximation [Method_{TI}; shown as gray lines in Fig. 7(a); normalized to have the same value for the devices with d_{emission} of 55 nm] fails to match the experimental results, demonstrating the importance of using the advanced model (Method_{full}) [22] adopted in this work, which includes the effect of SPP modes as well as other loss channels. In either case, it is clearly confirmed that the relative effect of d_{emission} behaves in a quite different and non-trivial manner even for a relatively small variation in d_{cap} . Based on these results, one may conclude that it is essential to optimize d_{emission} in conjunction with a given d_{cap} to utilize the full potential of TrOLEDs. With this approach, TrOLEDs can be realized with both high transmittance and efficiency, which are typically known to have a trade-off relationship [13, 15]. TrOLEDs with (d_{cap} , d_{emission}) given at (15 nm, 55 nm) and (30 nm, 55-80 nm) are good examples; their T_{OLED} 's are quite high and even close to 80%, yet their $\text{EQE}_{\text{total}}$ values are only slightly smaller than that of the TrOLEDs with (d_{cap} , d_{emission}) given at (40 nm, 80 nm), which has a T_{OLED} below 70%.

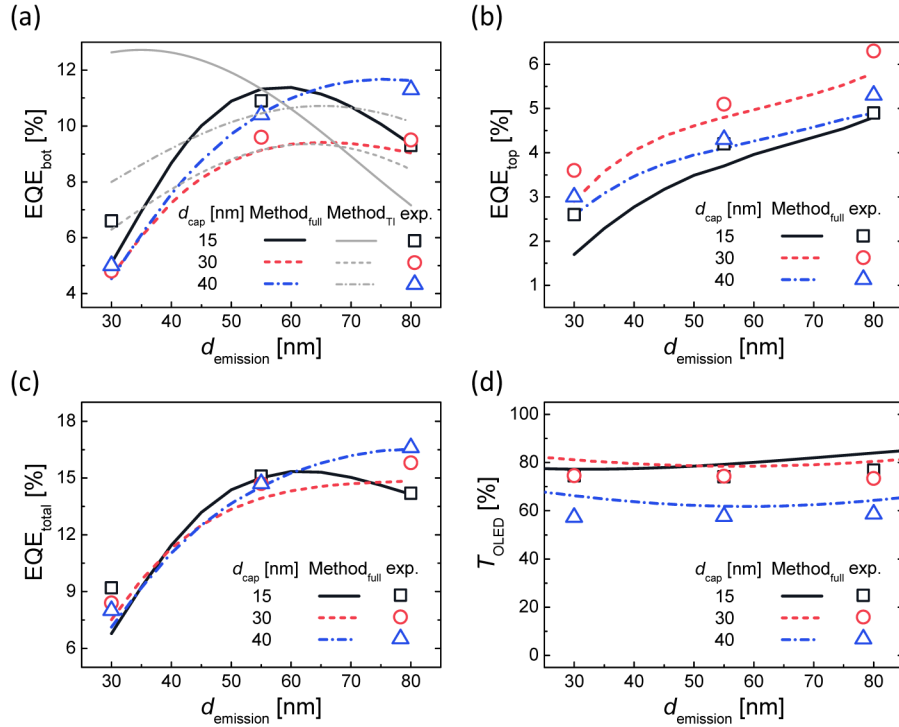


Fig. 7. External quantum efficiency for (a) bottom emission and (b) top emission, (c) as well as the sum of both directions and (d) the transmittance of TrOLEDs. The data were obtained by experiment (symbols) and optical simulation (lines) based on the classical dipole model (Method_{full}) [22] or on two-beam interference method described in Section 3.1 (Method_{TI}).

4. Conclusion

We proposed a strategy for achieving highly efficient TrOLEDs. Unlike opaque OLEDs, in which the location of the optimal emission zone (d_{emission}) is fixed with respect to the organic/metal electrode interface, it was shown that it has to be adjusted in accordance with the capping layer design in TrOLEDs mainly due to the associated phase change for reflection from the top cathode structure, which turns out to be more significant for the capping layer thickness (d_{cap}) near the value leading to high transmittance (T_{top}). With the optimal emission zone position found for a given d_{cap} , $\text{EQE}_{\text{total}}$ and transmittance values as high as 15% and 80%, respectively, were realized simultaneously for TrOLEDs based on Ir(ppy)₃ emitters. It was also shown that the effect of SPP loss from thin metal electrodes should also be taken into account to correctly describe the full scaling behavior of TrOLEDs over d_{cap} and d_{emission} as key design parameters. We believe the present work provides a rational guideline for the balanced design of TrOLEDs, opening up a way to unlock their full potential.

Acknowledgments

This work was supported by a National Research Foundation of Korea (NRF) grant funded by the Korea government (MSIP) (CAFDC 4-1, NRF-2007-0056090; NRF-2014R1A2A1A11052860). The authors are grateful to Samsung Display Corporation for funding through the KAIST Samsung Display Research Center Program.